Fault Diagnosis of Civil Engineering Structures using the Bond Graph Approach

Abbas Moustafa[†], Matthew Daigle[‡], Indranil Roychoudhury[‡], Chris Shantz[†], Gautam Biswas[‡], Sankaran Mahadevan[†], Xenofon Koutsoukos[‡]

[†]Department of Civil and Environmental Engineering, Vanderbilt University, Nashville TN 37235, USA

[‡]Department of Electrical Engineering and Computer Science, Vanderbilt University, Nashville TN 37235, USA

{abbas.m.moustafa, matthew.j.daigle, indranil.roychoudhury, chris.shantz, gautam.biswas, sankaran.mahadevan, xenofon.koutsoukos}@vanderbilt.edu

Abstract

This paper develops a fault diagnosis methodology for civil engineering structures based on the bond graph approach. The bond graph theory provides a modeling framework that includes parametric models of the physical system and the sensors. Structural faults are modeled as abrupt or gradual damage in structural components. Sensor faults are modeled as biases or drifts from true measurements. Fault detection uses a statistical method to identify significant deviations of measurements from nominal behavior of the structure. Fault isolation is carried out by comparing predicted effects of hypothesized faults with observed behavior of the structure. Numerical illustrations of fault diagnosis of a frame structure driven by time-varying loads are provided.

Introduction

Damage identification and health monitoring of civil engineering structures have received significant research attention worldwide (Doebling *et al*., 1998, Peeters & Roeck 2001, Chang *et al*., 2003). Diagnosing faulty behavior in these structures is crucial to their safe operation, and developing robust damage detection methodologies is a challenging problem. Damage detection schemes can be grouped into model-based and signal-driven methods. In model-based methods, the change in the system parameters, such as the structure's natural frequencies, mode shapes, and structural members' stiffness or damping coefficients are employed to characterize damage. Examples of model-based damage identification techniques include the ARX, ARMAX and the Least Squares models (Wang & Haldar 1994 and Kathuda *et al*., 2005). Signal-driven methods deal mainly with statistical and numerical analysis of measurement data (Jiang & Mahadevan 2005, 2007). Realistic scenarios for damage detection will combine methods for early detection of the occurrence of the damage and then isolating the fault to components, such as a beam or a column in a building. More advanced methods will also quantify the size of the damage. This allows for repair of the damaged component before catastrophic failure.

Bond graphs (BG) are an explicit topological modeling tool for capturing the common energy structure of systems (Rosenberg and Karnopp 1983). It is based on modeling energy flow between system components and inherently enforces continuity of power and conservation of energy. Bond graphs provide a systematic framework for building consistent and well constrained models of dynamic physical systems across multiple domains that include electrical, mechanical, hydraulic and thermal systems. The topological structure of BG models causality constraints that provide the mechanisms for effective and efficient fault diagnosis based on cause and effect analysis.

Our diagnosis algorithm is based on the TRANSCEND diagnosis framework (Mosterman & Biswas 1999). The diagnosis models, temporal causal graphs (TCGs), are derived systematically from BG models and provide the temporal and causal relations between deviant observations made on the system during its operation and hypothesized faults. Residuals are computed as deviations in measurements from nominal behavior. In an ideal or undamaged system the residuals should be zero. Nonzero residual values imply faults in the structural components or in the sensors. An abrupt fault is a sudden change in a system parameter (e.g., a sudden reduction in the stiffness or the damping of a structural member). Incipient faults result from slow variation in any of the system parameters over time that causes the system behavior to drift from its steady state (e.g., degradation or corrosion of steel bars over a long period of time). We assume faults are persistent.

This paper presents a methodology for applying bond graph theory to damage diagnosis for civil structures. The TRANSCEND algorithms are applied to a new domain, namely building structures. The paper focuses on detection and isolation of faults in structural components and sensors. For simplicity, we make the single fault assumption, but the methodology can be extended to multiple faults (Daigle *et al*. 2006).

Modeling Methodology

Model-based diagnosis methodologies require system models that accurately represent system dynamics and also link faulty behaviors to components of the model. We adopt the bond graph modeling framework that provides both these features and present a methodology for modeling multi-story building structures.

Bond graph models are constructed using the Fault Adaptive Control Technology (FACT) system (Manders *et al*. 2006) within the Generic Modeling Environment (GME) software developed at Vanderbilt University (GME-5 2005). MATLAB Simulink® models are automatically constructed from the bond graph models in GME using the tools described in (Roychoudhury *et al*. 2007).

Modeling Building Structures using Bond Graphs

Figure 1 shows a two-story frame structure. We first examine the effectiveness and accuracy of bond graph models of structures as compared to traditional structural dynamics modeling techniques. The equivalent lumped-mass model (two degree of freedom system) of the frame structure is shown in Figure 1(b). The lumped parameter elements of resistance (damping) (D_1, D_2), capacitance (stiffness) (k_1, k_2) and inductance (inertia) (m_1, m_2) are interconnected using energy conserving junctions producing the topological structure shown in Figure 2. Structural faults are represented by persistent, abrupt changes of the lumped parameter values. This bond graph represents the equations of motion of the frame structure in an implicit form. The bond graph is modular with each floor represented as a separate block. The blocks are connected through bond 5 to complete the frame structure. The sensors are also modeled as separate blocks for measuring displacements. Therefore, this modeling framework is easily extendible to *N*-story structures by duplicating the block of the second floor *N*-1 times.

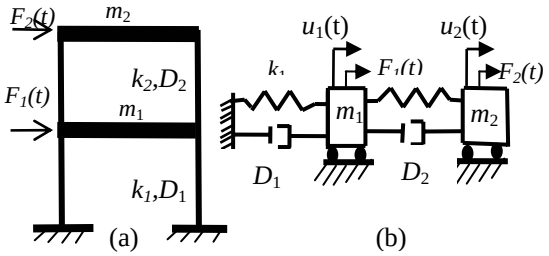

Figure1: (a) Frame building (b) Two-dof system

We first demonstrate the effectiveness of bond graphs to model these systems. To do this, we compute the dynamic responses of this system and compare them with those computed from the theory of structural dynamics. The structure is driven by the two sinusoidal forces $F_1(t) = 75\sin(9t)$ and $F_2(t) = 100\sin(9t)$ as shown in Figure 1. In our example, the stiffnesses of the structure are modeled by $k_1 = 30.70$ kN/m, $k_2 = 44.30$ kN/m, and the masses at the floor levels are $m_1 = 136$ N s^2/m, $m_2 = 66$ N s^2/m. The damping coefficients were modeled by the parameters $D_1 = 307$ Ns/m, $D_2 = 443$ Ns/m. The displacement, velocity and acceleration responses for the frame structure are computed using the derived simulation models and also by dynamic analysis using Duhamel's integral (Clough & Penzien 1993). Figure 3 depicts the displacement responses from the two methods. The figure shows a good match between responses computed using the two methods.

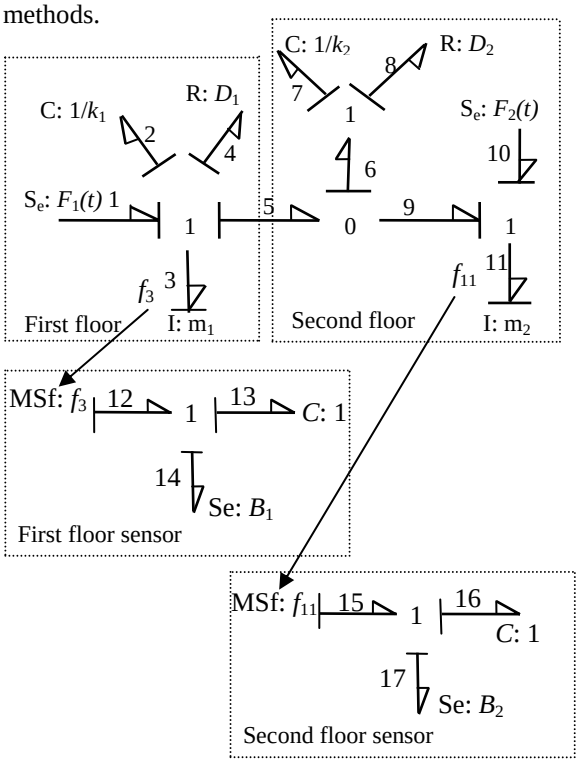

Figure 2: Bond graph model for the frame and the sensors

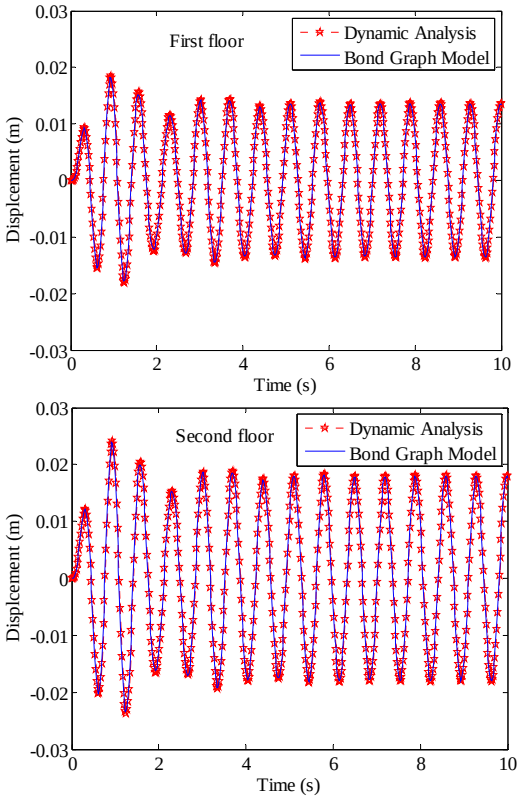

Figure 3: Dynamic response of the frame to sinusoidal loading

that the BG model provides sufficiently accurate results when compared to standard techniques from structural dynamics.

The bond graph model developed for the two-story frame structure was further examined when the structure is driven by the first horizontal component of the El Centro 1940 earthquake ground motion (SMDB 2000). The ground acceleration $\ddot{x}_g(t)$ is replaced by two horizontal forces $F_i(t) = -m_i \ddot{x}_g(t), i = 1,2$ acting on each floor. The displacement responses from the bond graph model and dynamic analysis is shown in Figure 4. Again, the structure responses show a good match compared with those obtained from the structural dynamics theory.

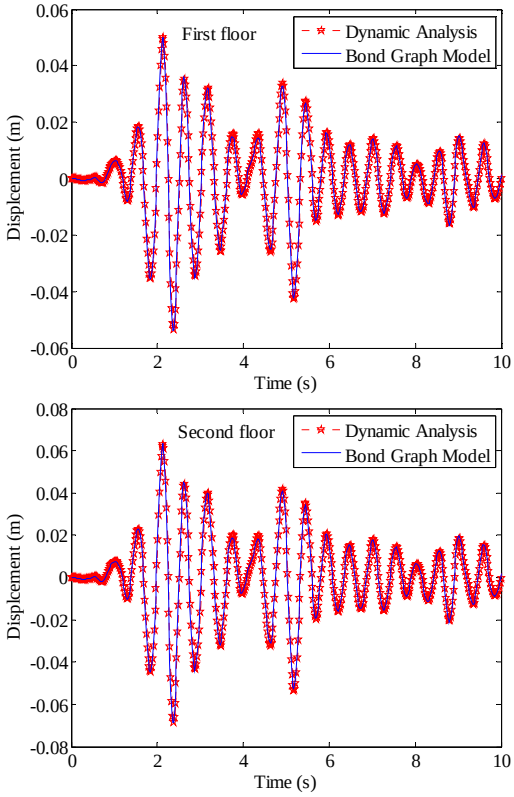

Figure 4: Dynamic response of the frame to earthquake acceleration

Modeling Sensors

From a practical point of view, deviations in measurements could result from damage in structural components or could also be attributed to sensor errors. For sensor errors, model-based identification models such as the finite element and the Least-Squares methods may not provide accurate results since these models do not account for sensor faults. On the other hand, bond graph models can easily model both the physical system and the sensors. Therefore, since faults are modeled as changes in the model parameters, bond graphs are capable of modeling faults in the structural components and sensors. This paper examines this issue by modeling sensors using bond graphs based upon the approach presented in (Daigle *et al.* 2006).

Faults in sensors could result in a bias or a drift in the measured values. Biased measurements are those measurements that deviate from their true value by a constant quantity *B*. Faults in sensor measurements could also result in a drift between the true value and the sensor measured value over time.

For a sensor measuring the displacement response, a bias fault implies that the actual measured displacement d_m is the sum of the true displacement d_t and the bias constant B. Nominally, B is zero. In the bond graph, the sensor is modeled using a modulated source of flow (MSf) and encapsulates the relation $d_m(t_i) = d_t(t_i) + B$, see Figure 2. As an example, consider the displacement sensor for the first floor. The effort associated with bond 12, e_{12} represents the measured displacement, the effort associated with bond 13 represents the true displacement, and the effort associated with bond 14 represents the bias quantity B. A C-element with $C = 1$ is included to integrate the true velocity to obtain true displacement. The effort balance of the 1-junction is $e_{12} = e_{13} + e_{14}$ where $e_{13}(t) = C\int f_{13}(\tau)d\tau = d_{13}(t)$ and $e_{14} = B_1$. This leads to $e_{12} = d_{13} + B_1$ or $d_m(t) = d_t(t) + B_1$.

In the case of drift, the measured response d_m is the sum of the true displacement d_t and the drift d_{drift}. The drift is a function that increases gradually with time. We model the drift using a linear function of time. Thus, $d_m(t) = d_t(t) + d_{dr}(t)$ or $d_m(t) = d_t(t) + gt$, where g is a constant representing the slope of the drift function. Again, the sensor is modeled in the same way as for bias, but the bias term is replaced by the drift function $d_{drift}(t) = g\,t$. Nominally, g is 0.

Fault Diagnosis Approach

The fault diagnosis methodology applied in this paper is a model-based method and consists of fault detection, symbol generation and qualitative isolation of faults. Figure 5 shows the overall architecture for the fault diagnosis approach. The parameter estimation of faulty components (fault identification) is not considered in the numerical examples. The details of the diagnosis procedures are provided below.

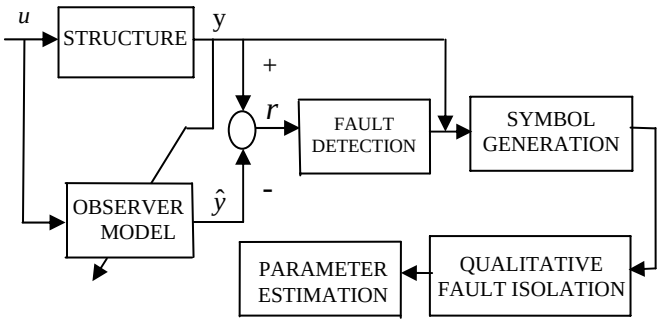

Figure 5: Diagnosis of dynamic systems

Fault Detection and Symbol Generation

The detection scheme is based on comparison of measurements from faulty and nominal structures. Herein, we distinguish between two distinct types of faults, namely, *abrupt* or sudden faults and *incipient* or degrading faults. Abrupt faults reflect a discontinuous reduction in any of the system parameters (e.g., a sudden reduction in the stiffness of a member of the structure). Incipient faults, on the other hand, represent a slow change in any of the model parameters. Abrupt faults can be expected to happen to structures subjected to short duration high amplitude loads such as blast loadings or strong motion earthquakes. Incipient faults could be expected to occur to structures in their steady state region such as structures subjected to vibrations from machineries.

The detection procedure is carried out by comparing the measurements of nominal (normal or undamaged) to faulty (damaged) measurements. This step leads to determining the residuals, the difference between observed and estimated behavior, which, when statistically significant, imply fault occurrence. The structure is considered to be faulty if the residual at any time point exceeds a predefined threshold value. When noise is included in the measurements, the Z-test is performed to examine if the structure is faulty or not.

From a practical and experimental point of view, the presence of noise in response measurements cannot be avoided. Noise implies uncertainty in the sensors which could be due to errors, inaccuracy, imprecision, or imperfection. When noise is present in the measurements of the structure responses, the estimation of the residual cannot be robustly carried out by simple subtraction of the data and comparing the residual with a predefined threshold value. Instead, a measure of the deviation of the residual from the ideal value (typically zero) is defined. The measure of the deviation at time t_i is defined by the average residual for the last N_2 measurement time points.

The decision whether the deviation is significant or not is based on a hypothesis test. In the present study we use the Z-test for this purpose (Biswas, *et al*., 2003). To perform the Z-test, the variance of the residual should be known. To approximate the conditions necessary for the Z-test, the variance of the signal is estimated but for a larger set of samples containing N_1 observation data points, where $N_1 >> N_2$. This approach is applied also to determine the slope of the deviation once detected.

The symbol generation follows the comparison of the measurements from nominal and faulty behavior. If the measurement of the faulty structure at a given point of time is above normal, a + symbol is assigned, and if below normal, a – symbol is assigned.

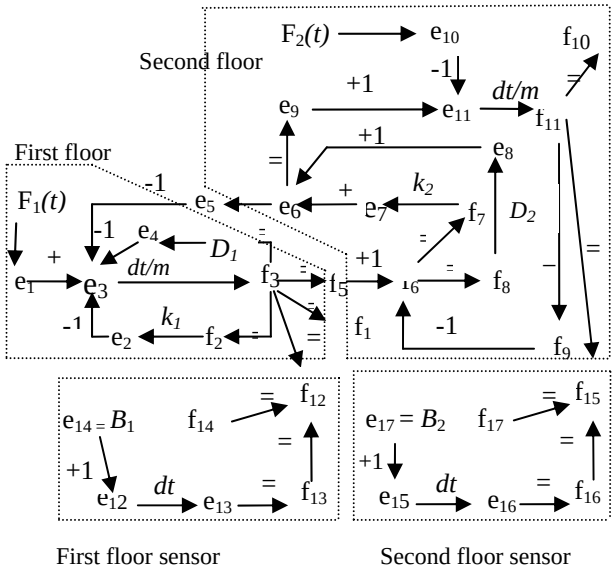

Figure 6: Temporal causal graph for the frame and the sensors

Fault Isolation

When faults are detected, fault isolation begins. The isolation scheme is based on the temporal causal graph (TCG), which is derived systematically from the bond graph model of the system (Mosterman & Biswas 1999). The TCG is derived based on the cause and effect relationships of the system variables and the constitutive equations of BG elements. For the two-story frame structure, the TCG is shown in Figure 6. The structure is first modeled using bond graphs and the TCG is constructed. The TCG links faults to their causal effects on measurements, called fault signatures. Fault signatures represent 0^{th} through k^{th} order derivative changes on a measurement residual at the point of fault occurrence. They provide the discriminatory power in the fault isolation approach.

The TCG is used to perform a backward propagation for the deviant measurement to generate the possible fault causes. This identifies a set of parameters that could be the reason for the fault. It also determines whether the cause is an increase or a decrease in the parameter. Some of these such as increase or decrease in the masses or increase in the stiffness or damping parameters are omitted. The qualitative fault isolation consists of two steps which are:

1. Perform forward propagation for each possible fault scenario determined in the previous step, to estimate the fault signature matrix. This matrix contains the qualitative effect of the change in the structure parameters (reduction - or increase +) on the measurements quantities. For instance, the signature of the stiffness parameter k_1 is derived from the TCG by assuming that k_1 decreases and tracking the effect of this on the displacements u_1 and u_2 and their derivatives. The signatures of other parameters are derived following the

same procedure. The fault signature for the frame structure of Figure 1 is provided in table 1.

2. Carry out progressive monitoring on each of these fault causes and the one that matches the fault signature is the actual fault.

Table 1: Fault signatures for the frame up to the first non zero direction of change

Fault	First floor displacement (u_1)	Second floor displacement (u_2)
k_1^-	00+	000+
k_2^-	00+	00-
D_1^-	00+	000+
D_2^-	00+	00-
B_1^+	+	0
B_2^+	0	+
B_1^-	-	0
B_2^-	0	-
dr_1^+	0+	00
dr_2^+	00	0+

The computed fault signatures of the frame structure are shown in Table 1. We only show the signature up to the first nonzero direction of change. Faults which produce discontinuities on the measurements (0^{th} order changes) provide additional discriminatory power. Higher order effects eventually manifest as first order effects, and since we can only measure magnitude and slope reliably, only the first change (and whether it was discontinuous) is useful. Since we measure displacement, the fault signatures represent a qualitative measure that reflects how a displacement observation could be affected by a change (reduction or increase) in one of the structure parameters. For instance, to derive the fault signature of the stiffness of the first floor k_1, a forward propagation is performed using the TCG of Figure 6 by tracing the qualitative effect of a decrease in k_1 on the response measurements u_1 and u_2. The signature is found to affect the second derivative of u_1 and the third derivative of u_2 and thus its signatures are 00+ and 000+, respectively. Signatures of other parameters are generated following the same procedure, described in detail in (Mosterman &Biswas 1999). It is observed from the table that the fault in the stiffness parameter of the first and the second floors have different signatures on the measurements u_1 and u_2. Furthermore, the signature of a fault in the stiffness parameter k_1 is the same due to a fault in the damping parameter D_1. The same observation is valid for the stiffness and damping coefficient of the second floor. This observation is consistent since the reduction in the stiffness or in the damping coefficient implies damage to the columns of the same floor, and in practical situations, knowing this is enough.

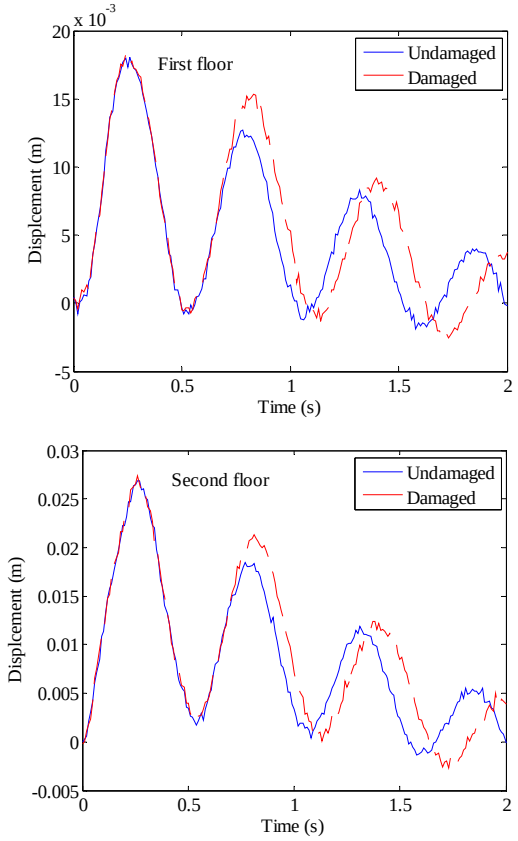

Figure 7: Noisy measurements (5% noise)

Numerical Examples

Two-story Building under Blast Loading

The two-story shear frame of Figure 1 is considered. This structure was studied by Wang & Haldar (1994) within the context of system identification of frame structures with unknown inputs. The structure is acted upon by a blast load of peak amplitude of 150 kN at t = 0 s decreasing linearly to zero at 2.0 s and applied at the second floor. The numerical values for stiffness, masses and damping considered previously are adopted in this example for simulating the theoretical response measurements for the undamaged and damaged structure. The displacement, velocity and acceleration responses at the two floors are computed using the simulation model generated from the bond graph. The possible fault causes considered include faults in the structural components (k_1, k_2, D_1, D_2) and bias (B_1, B_2) or drift (dr_1, dr_2) in the sensors.

Table 2: Natural frequencies of undamaged and damaged structure (Rad/s)

	Undamaged structure	Damaged structure (20 %)	
		k_1 damaged	k_2 damaged
ω_1	11.83	10.68 (9.72 %)	11.69 (1.18 %)
ω_2	32.91	32.61 (0.91 %)	29.78 (9.51 %)

The sampling time of the simulated responses was taken as 0.01 s. For the damaged structure, reductions of 10 % and 20 % in the parameters k_1, k_2, D_1 and D_2 were used for the experimental study. Table 1 summarizes the first two natural frequencies for the undamaged and the damaged structure due to damage of 20 % in the stiffness parameters. The table summarizes also the associated percentage reduction in natural frequencies. Figure 7 shows the theoretical displacement measurements for the undamaged and damaged structure.

Faults in Structural Components

We first consider damage in the columns of the first floor. The fault is simulated by reducing the stiffness parameter k_1 at t = 0.60 s by 20 % and the theoretical measurements u_1 and u_2 were computed using the simulation model. The noise free displacements of the undamaged and damaged structures were used as observations. Damage is considered to occur if the displacement measurements deviate by more than 5 % of the nominal values. The diagnosis model detects a fault at 0.70 s due to deviation in u_1 exceeding the threshold quantity adopted. The displacement u_2 deviates at 0.76 s. The backward propagation determines that the cause for the fault could be due to reduction in the stiffness parameters k_1 and k_2 or the damping coefficients D_1 and D_2 or due to increase in the masses m_1 *and* m_2. In this study, the possibility of faults occurring due to increases in the masses is eliminated since masses are assumed to remain unchanged.

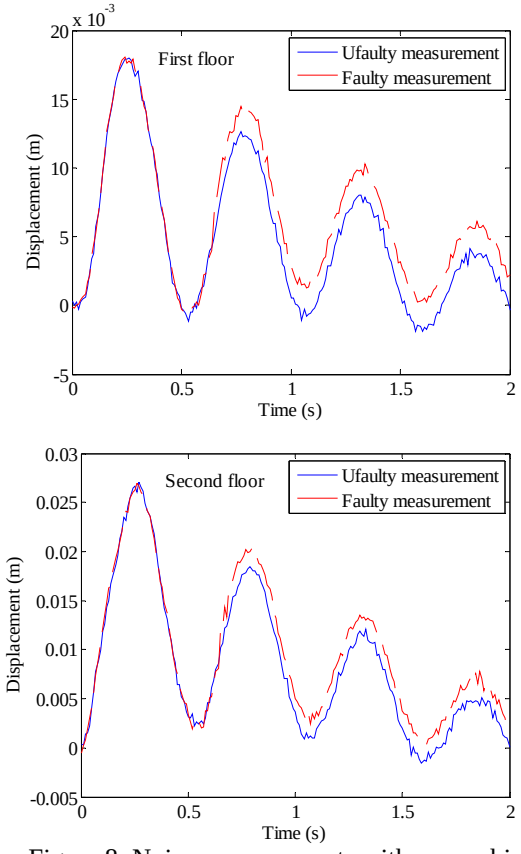

Figure 8: Noisy measurements with sensor bias

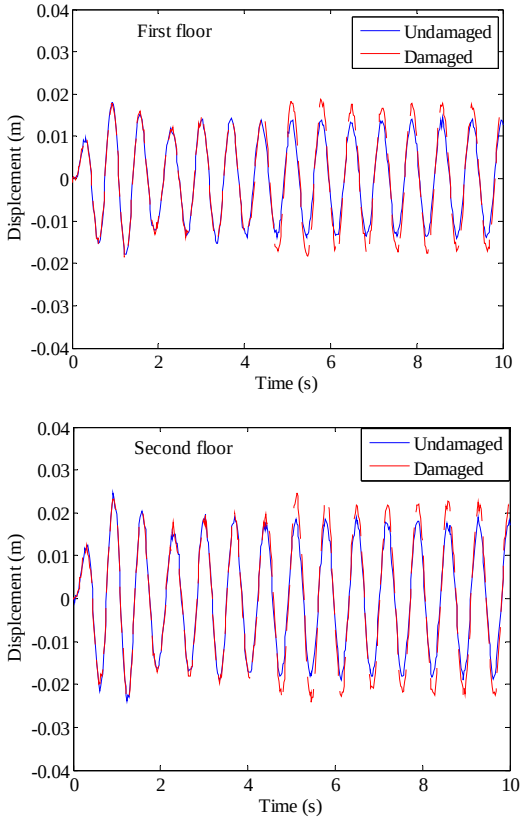

Figure 9: Noisy measurements (abrupt fault)

Table 3: Diagnosis results for the frame structure

Fault	Injection time (s)	Detection and diagnosis time
k_1^-	0.60 (20%)	u_1 deviates, 0.73, u_2 deviates 0.76 k_1^- or D_1^-
k_2^-	0.60 (20%)	u_2 deviates, 0.68, u_1 deviates 0.70 k_2^- or D_2^-
D_1^-	0.55 (20%)	u_2 deviates, 0.89, u_1 deviates 0.91 k_1^- or D_1^-
D_2^-	0.55 (20%)	u_2 deviates, 0.88, u_1 deviates 1.15 k_2^- or D_2^-
B_1^+	0.65 (0.002 m)	u_1 deviates, 0.68
B_2^+	0.65 (0.002 m)	u_2 deviates, 0.68

The forward propagations for reduction in the parameters k_1 or D_1 lead to the second derivatives of u_1 and u_2 above normal (00+). Similarly, the signature of reduction in k_2 or D_2 is accompanied by $\ddot{u}_1$ below normal (00-) and $\ddot{u}_2$ above normal (00+), see table 1. Comparing these signatures with the fault signature in Table 1, the fault is

identified in the columns of the first floor (due to reduction in either k_1 or D_1). A similar analysis with a reduction of 20 % in the damping coefficient D_1 was also carried out and the progressive monitoring leads to identifying the damage in the columns of the first floor. It is to be noted that the diagnosis model successfully isolates the fault to be in the columns of the first floor or the second floor. From engineering point of view, this is considered to be sufficient since damage in the columns implies reductions in stiffness and damping. The inspection that follows this step determines the location of the damage and necessary repair.

To address the issue of noise in measurements, a numerically generated stationary Gaussian white noise with zero mean and intensity 5 % of the root-mean-square values of the displacement at first floor is added to the theoretical responses. With the noise included in the response data, the structure is again diagnosed and some of these results are in Table 3 and Figures. 7-8. Herein, the Z-test is employed with the mean residual adopted in detecting the fault. In the numerical analyses, the parameters N_1, N_2, α are taken as 50, 5 and 1.0, respectively. By injecting a fault of 20 % reduction in the stiffness parameter k_1 and for a noise level of 5 %, the fault was detected at 0.73 s due to deviation on u_1 and u_2 deviates at 0.76 s (for noise free the fault was detected at 0.70 s). This implies that the presence of noise in the measurements may result in predicting the fault at a different time compared with the case of noise free measurements. The diagnosis model successfully detects and isolates the fault source to be in the stiffness or the damping coefficient of the first floor.

Faults in Sensors

We consider sensor faults modeled as bias in the measurements. We inject a bias of 0.002 m to the displacement at the first floor at 0.65 s. The true and faulty measurements at the first floor with noise included are shown in Figure 8. A similar analysis was carried out for a bias in the second sensor, see Figure 8. The fault signatures for individual biased measurements B_1 and B_2 are provided in Table 1. The signature of the bias in one sensor on the displacement measured by the same sensor is +. The bias or fault in one of the sensors has no effect on the other sensor which is physically true. In bond graph setting there is no path that connects the element source that simulates the bias element in one sensor (e.g., $S_e : B_1$) and the measurement in the other sensor (f_{13}) and therefore the signature is 0. For the bias B_1, the diagnosis model successfully detects the fault to be in the first sensor at 0.68 s. For the noise free measurements, the fault was identified at 0.65 s. A similar analysis with bias in the second sensor was carried out and the diagnosis model successfully detects the fault to be in the second sensor, see Table 3.

Two-story Building under Sinusoidal Load

To examine the applicability of the diagnosis model developed in this paper to alternative external loading conditions we reconsider the frame structure of Figure 1. The structure is assumed to be subjected to the sinusoidal forces $F_1(t) = 75\sin(9t)$ and $F_2(t) = 100\sin(9t)$ as shown in Figure 1(a). The frequency of the driving forces is selected to be close to the first natural frequency of the undamaged structure. The total duration of the input is taken as 10.0 s. In the previous example, the damage was introduced by decreasing the structure stiffness or damping at a certain time by some value. In practical situations, it is possible that damage to the structural members may occur gradually over time and not suddenly. For this reason, this example examines modeling degrading faults. This aspect, to the best of our knowledge has not been considered earlier within the context of fault diagnosis of civil structures.

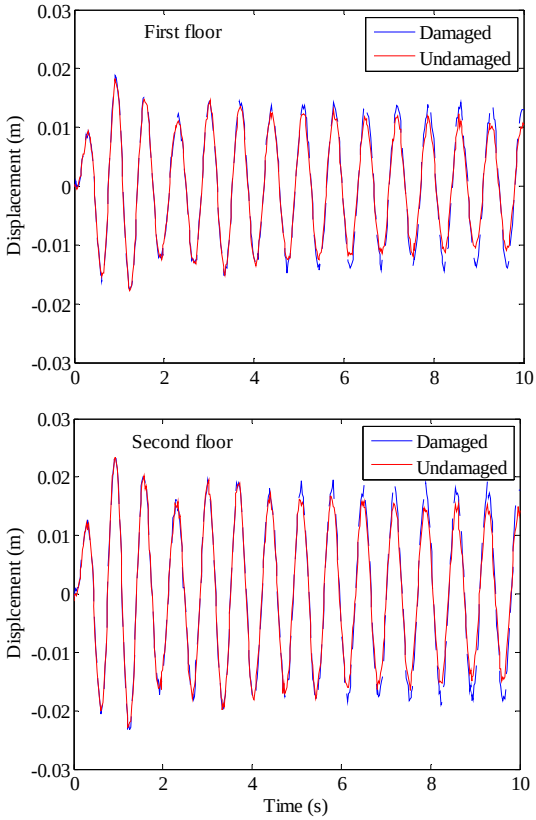

Figure 10: Noise free measurements (degrading fault)

We consider abrupt faults first. A reduction of 10 % in the stiffness parameter k_1 is applied at $t = 4.0$ s and the simulation model is used to generate the displacement measurements at the floors levels. Figure 9 shows the noisy displacement measurements for the undamaged and the damaged structure. The damage was detected at 4.10 s for the noise free measurements and at 4.16 s for the noisy measurements due to deviation in u_1. The numerical values for N_1, N_2 and α were taken as in the previous Example. Comparing the fault signatures of Table 1 and the measurements variation, it is seen that the damaged parameter is either k_1 or D_1 . Similar analysis was also obtained when the damage was introduced to the stiffness of the second floor and the diagnosis model detects the fault and isolates k_2 or D_2 as the damaged cause.

In the above analysis, the structure damage was modeled by a sudden reduction of 10 % in the stiffness parame-

ter k_1 at $t = 4.0$ s. To model a degrading damage, i.e., slowly varying damage to the structure, we introduce a linear reduction to the stiffness of the first floor. The damage represents a uniform reduction of 15 % in the parameter k_1 over the time period 3.0 to 10.0 s. Again, the structure displacement response for the damaged structure was simulated using the simulation model (see Figure 10). The diagnosis algorithm detects the damage at $t = 5.32$ s and the defect is in the columns of the first floor.

Conclusions

This paper develops a fault diagnosis methodology for civil engineering structures based on a qualitative approach to fault isolation. The paper focuses on fault detection and qualitative isolation of defected structural and sensor components. The proposed diagnosis scheme models sensors using bond graph components and therefore is capable of detecting and isolating faults in sensors as well. In this context, it may be emphasized that alternative damage diagnosis techniques such as ARX, ARMAX and the least-squares models do not account for sensor faults.

For verification purposes, both noise-free and noisy response measurements were considered. The advantage of the present diagnosis scheme is the isolation of faulty components with less computation compared to solely quantitative diagnosis methods such as ARX, ARMAX and the least-squares approach. In the present paper, fault diagnosis of a two-story frame structure was studied. The diagnosis of larger and complex structures is of interest. Furthermore, the diagnosis algorithm can be further improved by including a least-squares scheme to quantify the fault size of the isolated faulty component.

In the present study, physical dynamic systems such as frame structures were modeled using shear frame models. The use of more accurate models for continuous systems taking into account translational and rotational degrees of freedom is of significant interest. It is also of interest to investigate multiple fault scenarios.

References

Biswas, G., Simon, G., Mahadevan, N., Narasimhan, S., Ramirez, J., Karsai, G., 2003, A robust method for hybrid diagnosis of complex systems, In Proc. of the 5th Symposium on Fault Detection, Supervision and Safety for Technical Processes, pages 1125-1131, Washington, DC, June 2003.

Chang, P.C., Flatau, A., Liu, S.C., 2003, Review paper: Health monitoring of civil infrastructure, *Structural Health monitoring*, 2:3, 257-267.

Clough, R.W., Penzien, J., 1993, *Dynamics of structures*, McGraw-Hill, 2nd Edition, Tokyo.

Daigle, M., Koutsoukos, X., Biswas, G., 2006, Distributed diagnosis of coupled mobile robots, *2006 IEEE International Conference on Robotics and Automation*, 3787-3794.

Daigle, M., Koutsoukos, X., Biswas, G., 2006, Multiple fault diagnosis in complex physical systems, In *Proceedings of the 17th International Workshop on Principles of Diagnosis,*, 69-76.

Doebling, S.W., Farrar, C.R., Prime, M.B., 1998, A summary review of vibration-based damage identification methods, *The shock and vibration digest*, 30(2), 91-105.

GME-5 2005, A Generic Modeling Environment, GME 5 User's Manual, Vanderbilt University, http://www.isis.vanderbilt.edu.

Jiang, X., Adeli, H., 2007, Pseudospectra, MUSIC and dynamic wavelet neural network for damage detection of high-rise buildings, *International Journal for Numerical Methods in Engineering*, in press.

Jiang, X., Mahadevan, S., Adeli, H., 2007, Bayesian wavelet packet denoising for structural system identification, *Structural Control and Health Monitoring*, in press.

Katkhuda, H, Martinez, R., Haldar, A., 2005, Health assessment at local level with unknown input excitation, *Journal of Structural Engineering*, 131(6), 956-965.

Manders, E. J.; Biswas, G.; Mahadevan, N.; and Karsai, G 2006. Component-oriented modeling of hybrid dynamic systems using the Generic Modeling Environment. In *Proceedings of the 4th Workshop on Model-Based Development of Computer Based Systems*.

Mosterman, P.J., Biswas, G., 1999, Diagnosis of continuous valued systems in transient operating regions, *IEEE Transactions, Man, and Cybernetics-Part A*, 29(6).

Peeters, B., Roeck, G.D., 2001, Stochastic system identification for operational modal analysis: A review, *Journal of Dynamic Systems, Measurements, and control*, 123, 659-667.

Rosenberg R.C., and Karnopp D.C., 1983, *Introduction to physical system dynamics*: McGraw-Hill, New York.

Roychoudhury, I.; Daigle, M.; Biswas, G.; Koutsoukos, X.; and Mosterman, P. J. 2007. A Method for Efficient Simulation of Hybrid Bond Graphs. In *Proceedings of the International Conference on Bond Graph Modeling (ICBGM 2007)*,177-184.

SMDB, 2000, The Strong Motion Data-based, http://smdb.crustal.ucsb.edu, South California Earthquake center.

Wang D., Haldar, A., 1994, Element-level system identification with unknown input, *Journal of Engineering Mechanics*, 120(1), 159-176.